

# Velocity analysis using $AB$ semblance<sup>a</sup>

<sup>a</sup>Published in Geophysical Prospecting, v. 57, 311-321 (2009)

*Sergey Fomel*

## ABSTRACT

I derive and analyze an explicit formula for a generalized semblance attribute, which is suitable for velocity analysis of prestack seismic gathers with distinct amplitude trends. While the conventional semblance can be interpreted as squared correlation with a constant, the  $AB$  semblance is defined as a correlation with a trend. This measure is particularly attractive for analyzing class II AVO anomalies and converted waves. Analytical derivations and numerical experiments show that the resolution of the  $AB$  semblance is approximately twice lower than that of the conventional semblance. However, this does not prevent it from being an effective attribute. I use synthetic and field data examples to demonstrate the improvements in velocity analysis from  $AB$  semblance.

## INTRODUCTION

Since its introduction by Taner and Koehler (1969), the semblance measure has been an indispensable tool for velocity analysis of seismic records. Conventional velocity analysis of seismic gathers scans different values of effective moveout velocity, computes semblance of flattened gathers and generates velocity spectra for later velocity picking (Yilmaz, 2000).

While effective in most practical situations, semblance becomes troublesome in the case of strong variation of amplitudes along seismic events (Sarkar et al., 2001). A particular example is class II AVO anomalies (Rutherford and Williams, 1989) that cause seismic amplitudes to go through a polarity reversal. To address this problem, Ratcliffe and Adler (2000) and Sarkar et al. (2001, 2002) developed algorithms for correcting the semblance measurement for amplitude variations.

In this paper, I interpret the semblance attribute as a correlation with a constant and derive an explicit mathematical expression for the measure which corresponds to correlation with an amplitude trend. This measure is equivalent to  $AB$  semblance proposed by Sarkar et al. (2001, 2002). It reduces, in the case of constant amplitudes, to the conventional semblance. I analyze the statistics of the  $AB$  semblance attribute and quantify the loss of resolution associated with it. Numerical experiments with synthetic and field data demonstrate the effectiveness of the  $AB$  semblance as a robust velocity analysis attribute, which is applicable even in the presence of strong

amplitude variations and polarity reversals. Moreover, the ratio of the *AB* and conventional semblances serves as a useful AVO indicator attribute.

## THEORY

I start by interpreting the meaning of the conventional semblance attribute as a correlation with a constant. Next, I define *AB* semblance as a correlation with a trend and analyze its statistical properties.

### Semblance as correlation

The correlation coefficient  $\gamma$  between two sequences of numbers  $\mathbf{a} = a_1, a_2, \dots, a_N$  and  $\mathbf{b} = b_1, b_2, \dots, b_N$  is defined as

$$\gamma(\mathbf{a}, \mathbf{b}) = \frac{\mathbf{a} \cdot \mathbf{b}}{|\mathbf{a}| |\mathbf{b}|} = \frac{\sum_{i=1}^N a_i b_i}{\sqrt{\sum_{i=1}^N a_i^2} \sqrt{\sum_{i=1}^N b_i^2}} \quad (1)$$

The correlation coefficient is analogous to the cosine of the angle between two vectors  $\mathbf{a}$  and  $\mathbf{b}$ . It takes values in the range from  $-1$  to  $1$ . Taking a correlation of a sequence  $\mathbf{a}$  with a constant sequence  $\mathbf{c} = C, C, \dots, C$  produces a measure  $\beta$ , defined as

$$\beta(\mathbf{a}) = \gamma(\mathbf{a}, \mathbf{c}) = \frac{\sum_{i=1}^N a_i C}{\sqrt{\sum_{i=1}^N a_i^2} \sqrt{\sum_{i=1}^N C^2}} = \frac{\sum_{i=1}^N a_i}{\sqrt{N \sum_{i=1}^N a_i^2}} \quad (2)$$

Squaring the correlation with a constant yields the measure equivalent to semblance

$$\beta^2(\mathbf{a}) = \frac{\left( \sum_{i=1}^N a_i \right)^2}{N \sum_{i=1}^N a_i^2}. \quad (3)$$

Semblance is maximized when the sequence  $\mathbf{a}$  has a uniform distribution. When seismic amplitude is uniformly distributed along a moveout curve, the semblance of a horizontal slice through the gather will be maximized when the event is flattened. This fact is the basis of the conventional velocity analysis originally developed by Taner and Koehler (1969). The approach fails, however, when the amplitude variation is distinctly non-uniform.

### AB semblance: correlation with a trend

Suppose that the reference sequence has a trend  $b_i = A + B \phi_i$ , where  $\phi_i$  is a known function. The trend can be, for example, an expression of the *PP* reflection coefficient in Shuey's approximation (Shuey, 1985), where  $A$  and  $B$  are the AVO intercept and gradient,  $\phi_i = \sin^2 \theta_i$ , and  $\theta_i$  corresponds to the reflection angle at trace  $i$ . In examples of this paper, I use offset instead of angle. Relating offset and reflection angle can be done either by using approximate equations or by ray tracing once the velocity model is established.

Estimating  $A$  and  $B$  from least-square fitting of the trend amounts to the minimization of

$$F(A, B) = \sum_{i=1}^N (a_i - A - B \phi_i)^2 \quad (4)$$

Differentiating equation (4) with respect to  $A$  and  $B$ , setting the derivatives to zero, and solving the system of two linear equations produces the well-known linear fit equations

$$A = \frac{\sum_{i=1}^N \phi_i \sum_{i=1}^N a_i \phi_i - \sum_{i=1}^N \phi_i^2 \sum_{i=1}^N a_i}{\left( \sum_{i=1}^N \phi_i \right)^2 - N \sum_{i=1}^N \phi_i^2}, \quad (5)$$

$$B = \frac{\sum_{i=1}^N \phi_i \sum_{i=1}^N a_i - N \sum_{i=1}^N a_i \phi_i}{\left( \sum_{i=1}^N \phi_i \right)^2 - N \sum_{i=1}^N \phi_i^2}. \quad (6)$$

Substituting the trend  $b_i = A + B \phi_i$  with  $A$  and  $B$  defined from the least-squares equations (5) and (6) into the correlation coefficient equation (1) and squaring the result leads to equation

$$\alpha^2(\mathbf{a}) = \frac{2 \sum_{i=1}^N a_i \sum_{i=1}^N \phi_i \sum_{i=1}^N a_i \phi_i - \left( \sum_{i=1}^N a_i \right)^2 \sum_{i=1}^N \phi_i^2 - N \left( \sum_{i=1}^N a_i \phi_i \right)^2}{\sum_{i=1}^N a_i^2 \left[ \left( \sum_{i=1}^N \phi_i \right)^2 - N \sum_{i=1}^N \phi_i^2 \right]}. \quad (7)$$

Equation (7) generalizes the semblance measure  $\beta$  defined in equation (3) to a new measure  $\alpha$ . In the absence of a trend (when the numerator in equation (6) is zero),  $\alpha$  is equivalent to  $\beta$ .

Sarkar et al. (2001) defined semblance using a normalized least-squares objective

$$\alpha^2(\mathbf{a}) = 1 - \frac{F(A, B)}{\sum_{i=1}^N a_i^2}. \quad (8)$$

Substituting equations (5) and (6) into (8) is an alternative way of deriving equation (7). This is the *AB semblance* in terminology of Sarkar et al. (2001, 2002).

## Sensitivity analysis of *AB* semblance

Sarkar et al. (2001, 2002) observed a decrease of resolution in *AB* semblance in comparison with the conventional semblance when applying it on synthetic examples. The explicit equation (7) allows us to access the resolution limits of both methods by measuring their effect on random noise.

As shown in Appendix A, the semblance of a sequence of uncorrelated normally-distributed zero-mean noise samples has the expectation value of  $1/N$ , where  $N$  is the number of samples. The corresponding *AB* semblance has the expectation  $2/N$  or twice higher. Moreover, while the standard deviation of the conventional semblance decreases as  $1/N$ , the deviation of the *AB* semblance decreases as  $2/N$ . This analysis shows that the *AB* measurement is generally twice as sensitive to noise and has a twice lower resolution. This is the price one has to pay for the ability to handle amplitude trends.

## EXAMPLES

In this section, I demonstrate the behavior of *AB* semblance with a synthetic and a field data example.

### Synthetic example

Figure 1 shows two synthetic CMP gathers generated by applying inverse normal moveout with a variable moveout velocity and adding a modest amount of random noise. The first gather contains no amplitude variations, while the second gather contains a region of polarity reversal. Figure 2 shows velocity analysis panels using conventional semblance scans and the corresponding automatic velocity picks. The picking algorithm is explained in Appendix B. We can observe that the AVO anomaly causes a signal loss in the semblance measure, which in turn leads to inaccurate velocity picking. The *AB* semblance, on the other hand, is not affected much by the amplitude variations and allows for accurate velocity picking in both cases, as shown in Figure 3.

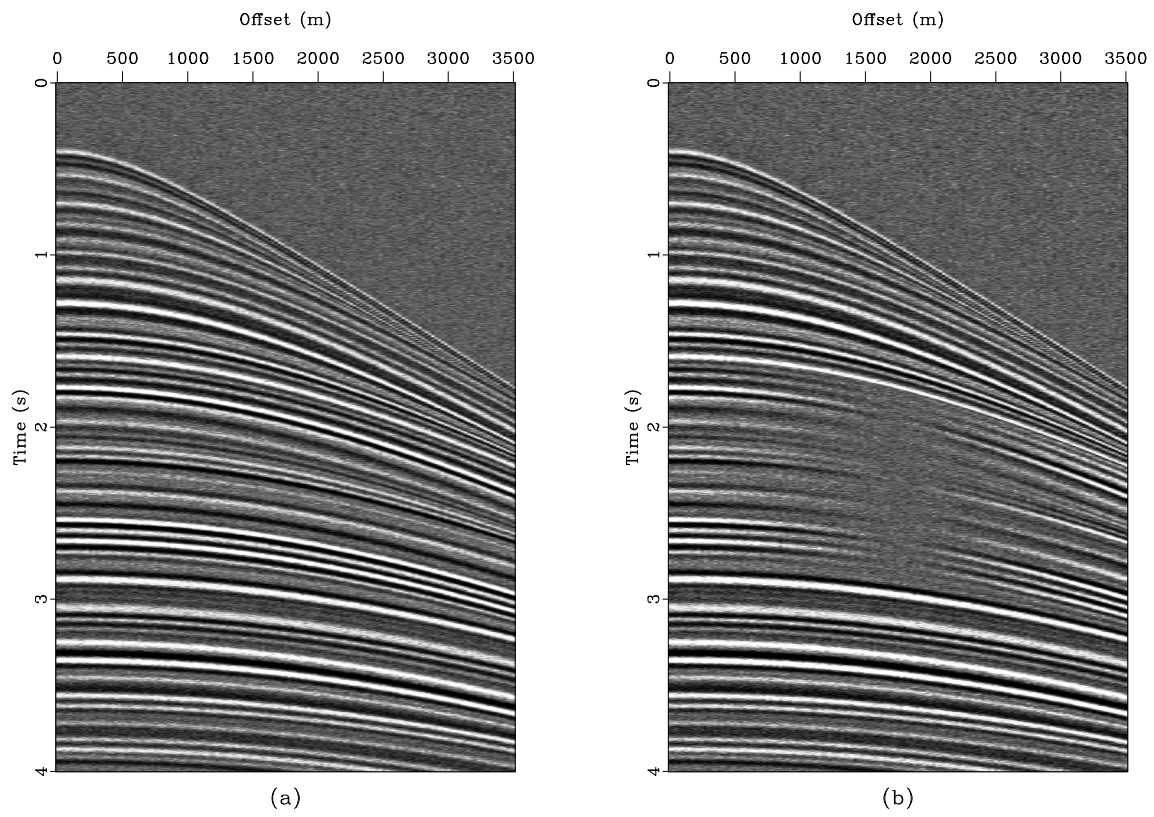


Figure 1: Synthetic CMP gathers. a: no AVO, b: AVO trend with polarity reversal in the middle section.

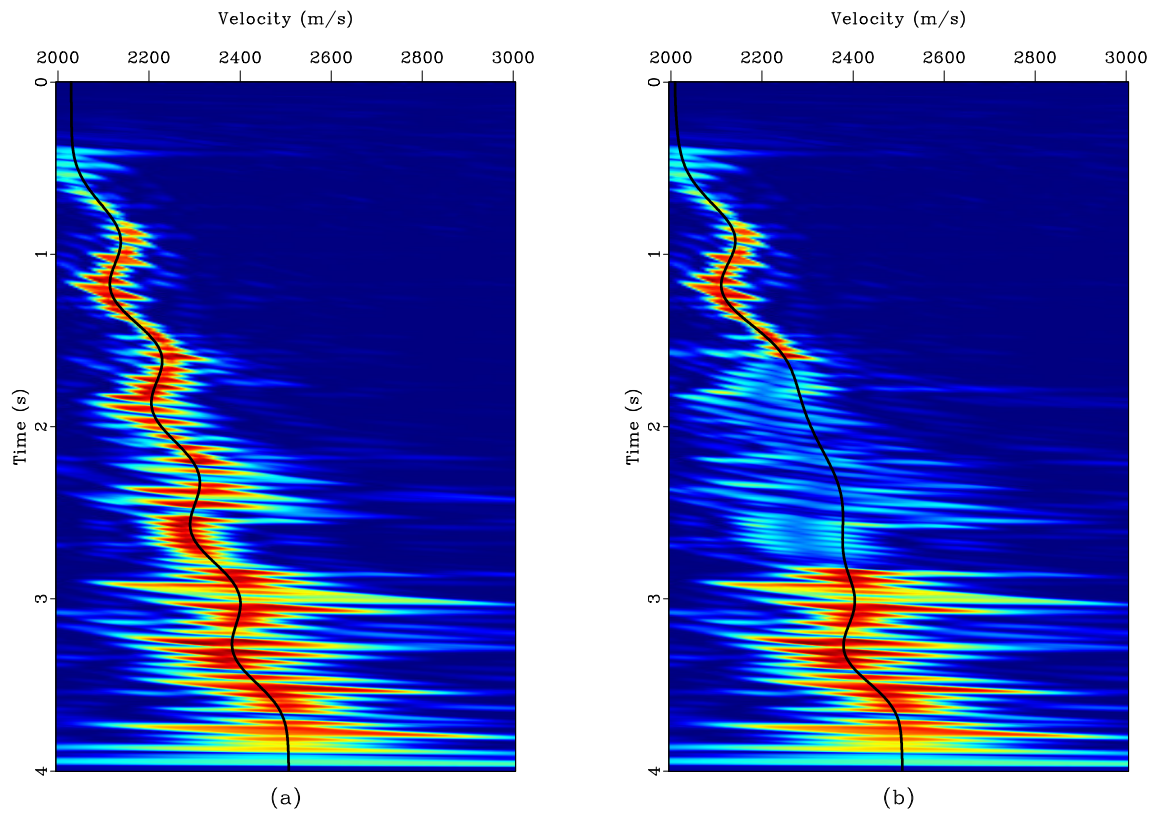


Figure 2: Conventional semblance scans for CMP gathers from Figure 1. Black curves indicate automatic velocity picks. The loss of signal in the right plot is caused by the AVO anomaly. a: no AVO, b: AVO trend with polarity reversal in the middle section.

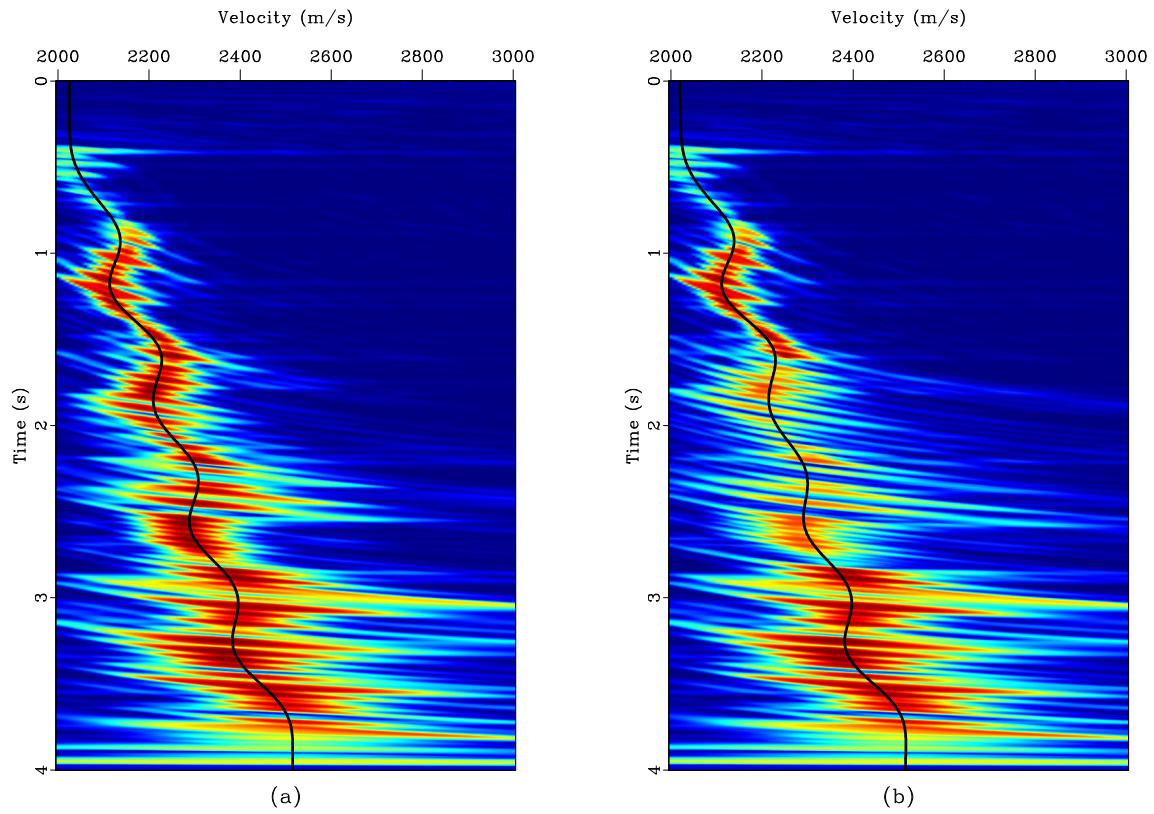


Figure 3: *AB* semblance scans for CMP gathers from Figure 1. Black curves indicate automatic velocity picks. Semblance remains strong despite the AVO anomaly. a: no AVO, b: AVO trend with polarity reversal in the middle section. Compare with Figure 2.

Figures 4 and 5 compare NMO-corrected gathers using velocities picked from the conventional and *AB* semblance scans respectively. While Figures 4a and 5a are virtually identical, the residual curvature evident in the anomalous region in Figure 4b disappears in Figure 5b, which clearly demonstrates the advantage of the *AB* approach. Figure 6 shows NMO-corrected gathers colored according to the AVO-indicator attribute, which I define as a ratio between the conventional and the *AB* semblances. The anomalous region is clearly visible in the attribute display.

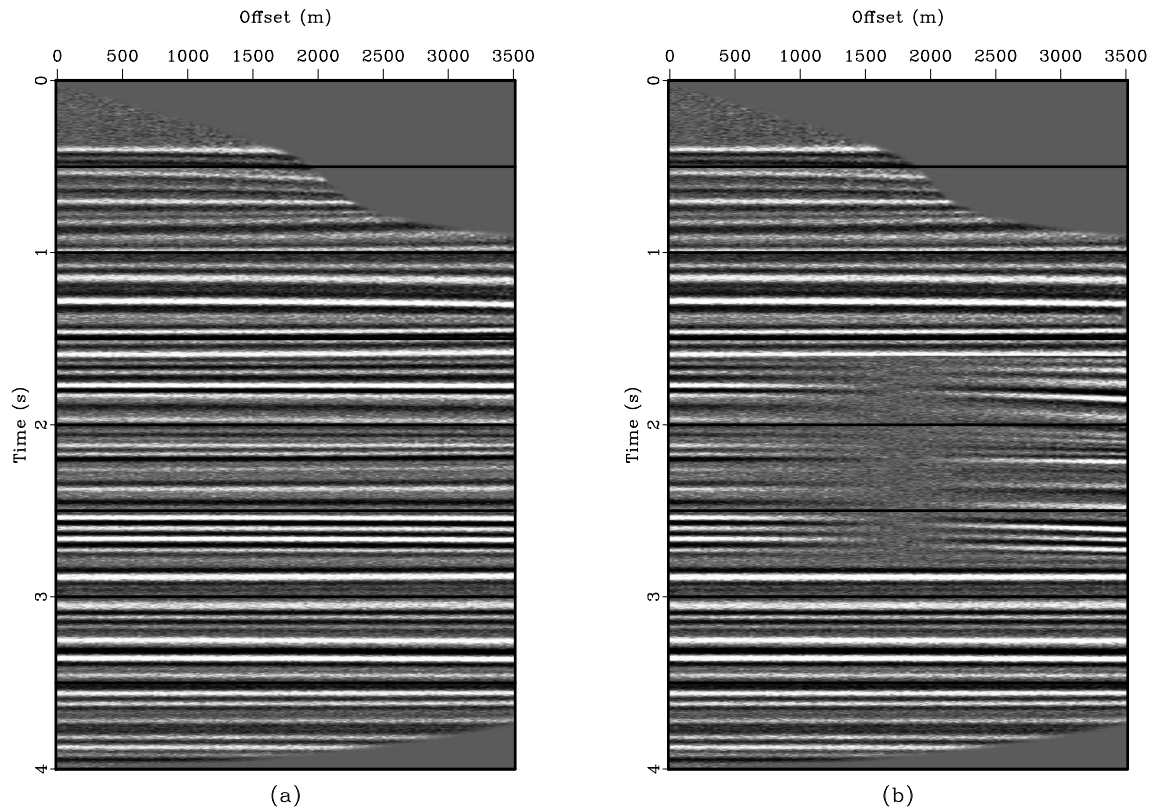


Figure 4: NMO-corrected CMP gathers from Figure 1 using velocity functions picked from conventional semblance in Figure 2.

## Field data example

For a field data example, I select a gather already processed by a seismic contractor. The gather, shown in Figure 7, exhibits a clear polarity reversal around 3.8 s. The polarity reversal is the apparent cause of a visible residual moveout artifact. In order to correct the residual curvature, I apply semblance-based analysis. The comparison between the conventional and the *AB* semblance is shown in Figure 8. Similarly to the synthetic example, the *AB* semblance provides a better indicator of the residual velocity for the curved event with anomalous amplitude. Figure 9 shows NMO-corrected gather using a velocity trend picked automatically from the *AB* analysis. The curved reflection event is successfully flattened.

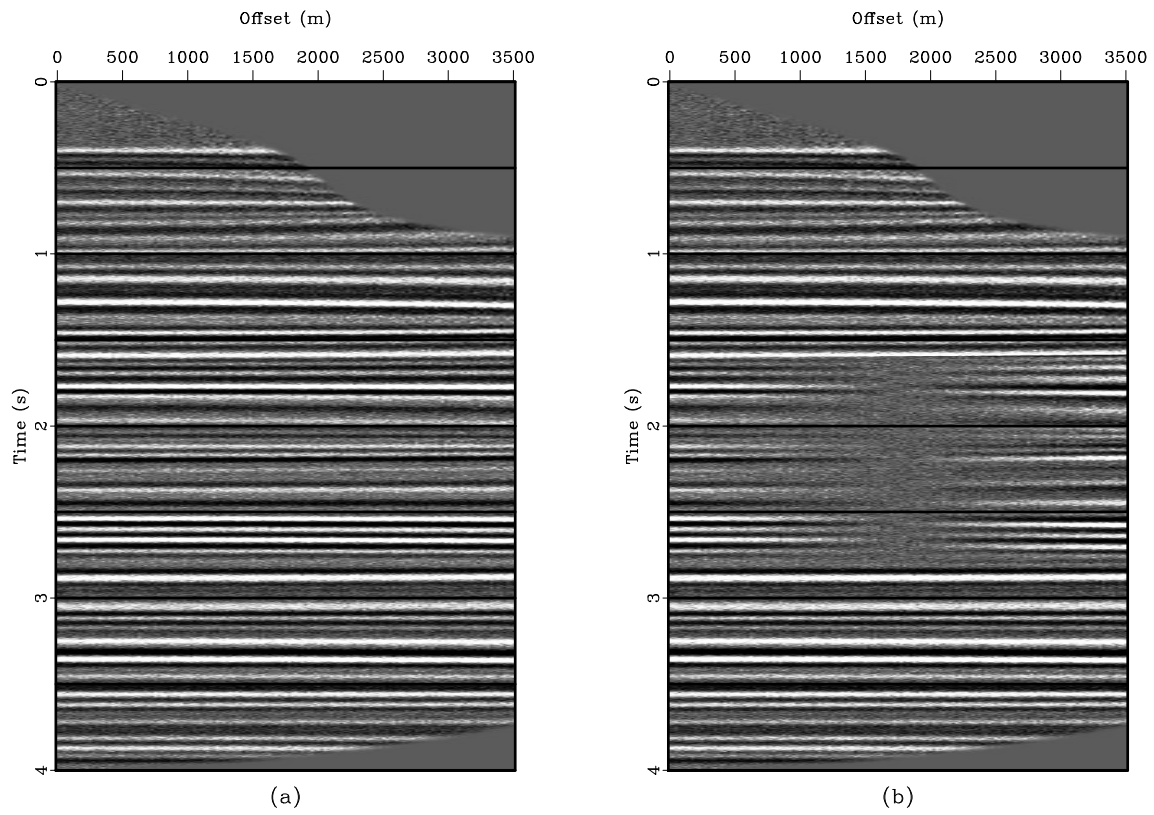


Figure 5: NMO-corrected CMP gathers from Figure 1 using velocity functions picked from *AB* semblance in Figure 3.

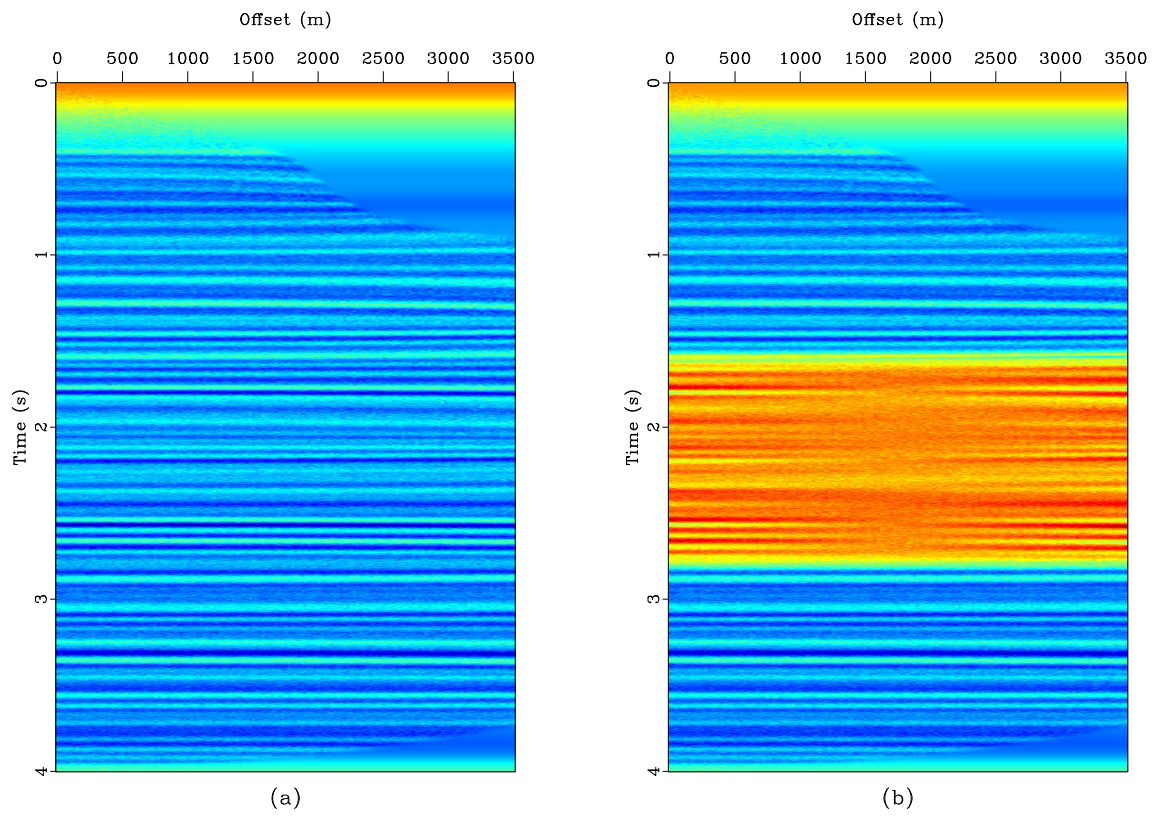


Figure 6: NMO-corrected CMP gathers from Figure 5 colored according to the AVO indication attribute.

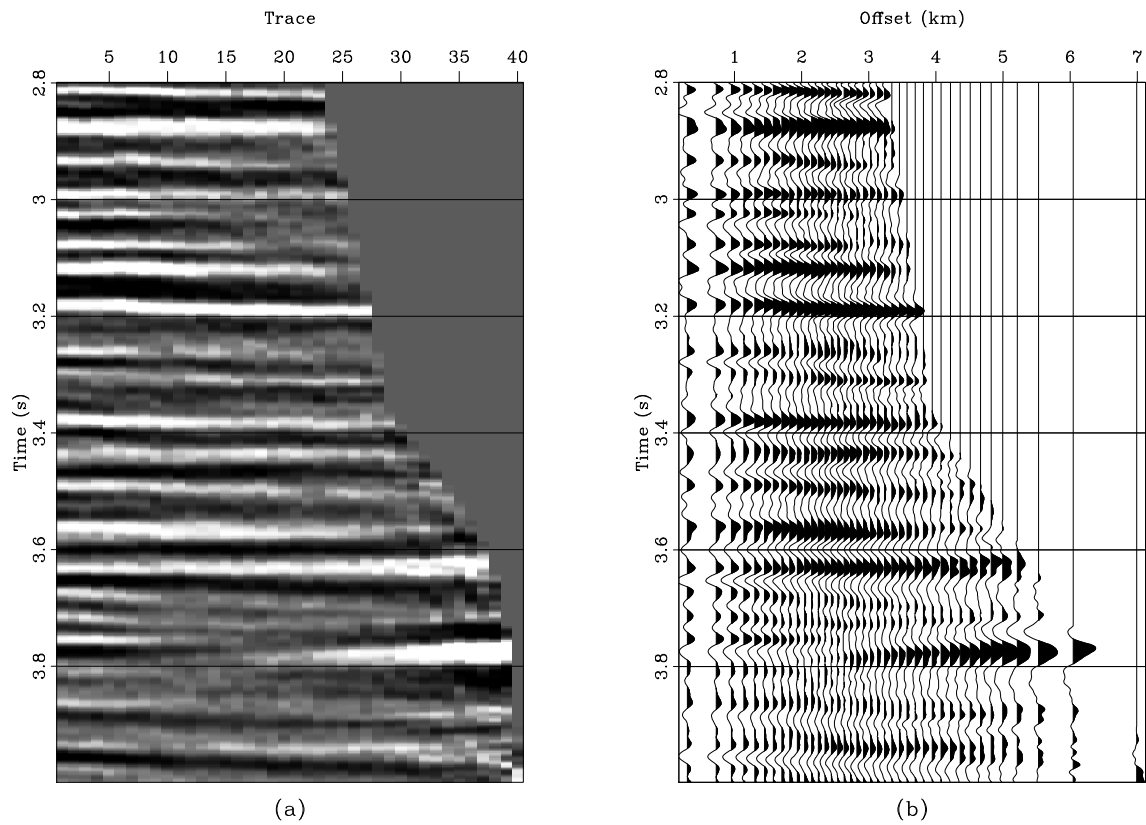


Figure 7: Input CMP gather after preprocessing. a: trace display, b: wiggle display.

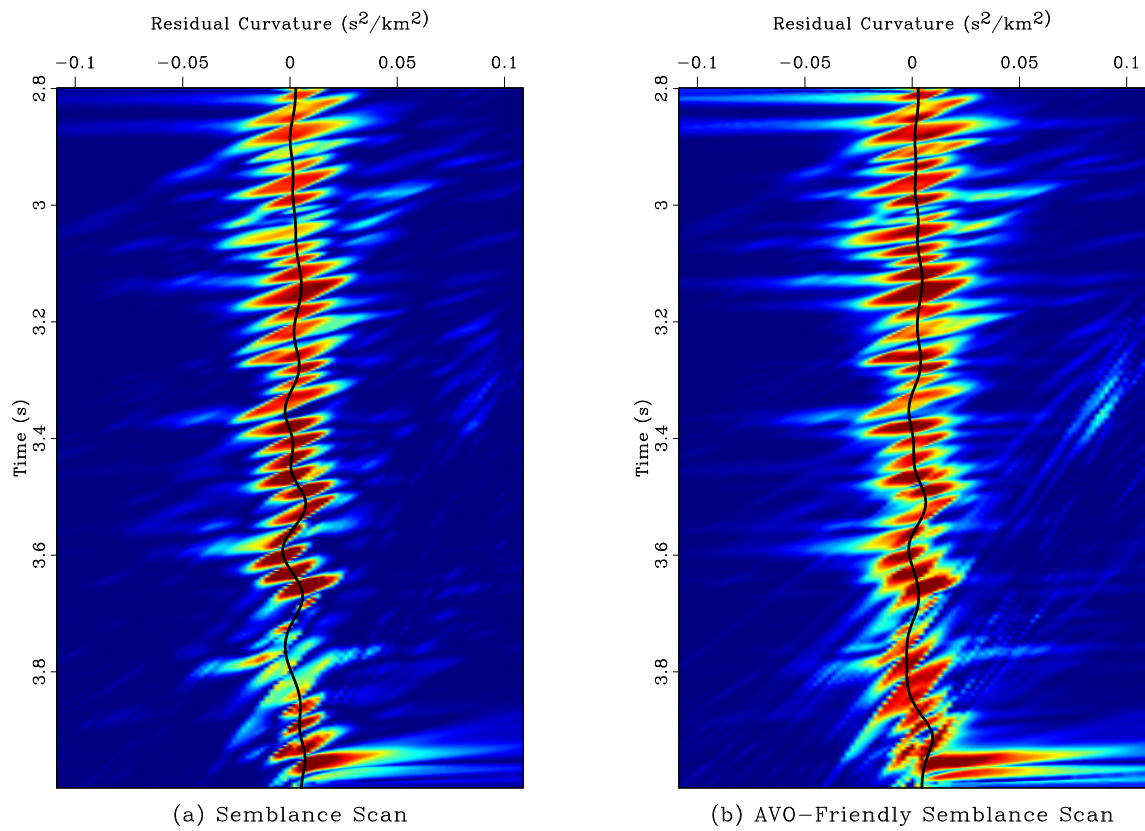


Figure 8: Residual moveout curvature scans using conventional semblance (a) and *AB* semblance (b). Black curves indicate automatically picked trends.

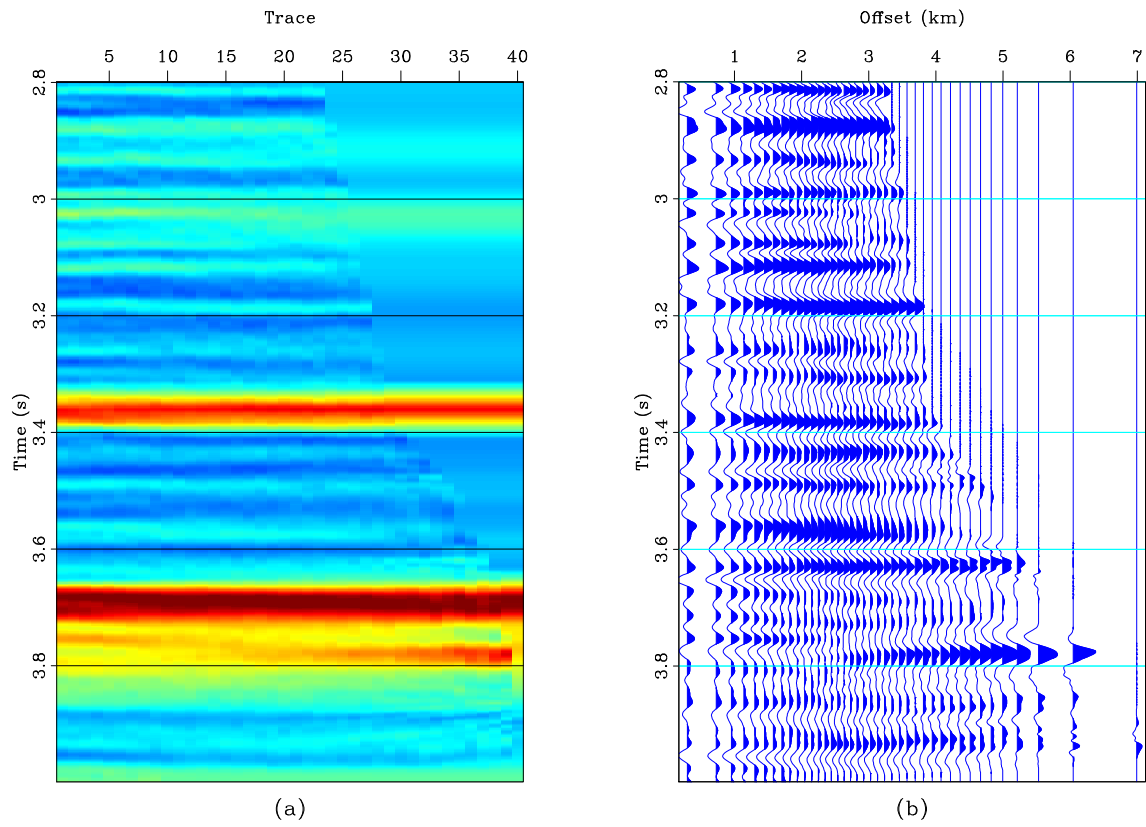


Figure 9: CMP gather from Figure 7 after residual normal moveout correction using trends picked from the *AB* semblance in Figure 8. a: trace display colored according to the AVO indicator attribute, b: wiggle display.

## CONCLUSIONS

If one interprets the conventional semblance as a correlation with a constant, the  $AB$  semblance is a correlation with an amplitude trend. I have derived an explicit expression for the  $AB$  semblance and analyzed it to quantify the observable loss of resolution. I have demonstrated the advantages of the  $AB$  semblance attribute using synthetic and field data examples. The ratio of the  $AB$  and conventional semblances serves as a useful AVO indicator attribute. The sensitivity of this attribute to non-linear variations in the amplitude trend can be a subject of further research. Further applications may also include velocity analysis of converted waves and seismic diffractions.

## ACKNOWLEDGMENTS

I would like to thank Tury Taner and Richard Uden for inspiring discussions and for providing the field data example.

This publication is authorized by the Director, Bureau of Economic Geology, The University of Texas at Austin.

## APPENDIX A

### STATISTICAL ANALYSIS OF SEMBLANCE MEASURES

In this appendix, I study the influence of noise on semblance measures. Let us assume that the signal  $\mathbf{a} = a_1, a_2, \dots, a_N$  is composed of random independent samples normally distributed with zero mean and  $\sigma^2$  variance. In this case, the mathematical expectation for the semblance measure (3) is

$$E[\beta^2(\mathbf{a})] = \frac{E\left[\left(\sum_{i=1}^N a_i\right)^2\right]}{E\left[N \sum_{i=1}^N a_i^2\right]} = \frac{\sum_{i=1}^N E[a_i^2]}{N \sum_{i=1}^N E[a_i^2]} = \frac{1}{N}. \quad (\text{A-1})$$

Correspondingly, the variance of the noise semblance is

$$\begin{aligned} V[\beta^2(\mathbf{a})] &= \frac{E\left[\left(\sum_{i=1}^N a_i\right)^4\right]}{E\left[\left(N \sum_{i=1}^N a_i^2\right)^2\right]} - \frac{1}{N^2} = \frac{\sum_{i=1}^N E[a_i^4] + 3 \sum_{i=1}^N \sum_{j \neq i} E[a_i^2 a_j^2]}{N^2 \left(\sum_{i=1}^N E[a_i^4] + \sum_{i=1}^N \sum_{j \neq i} E[a_i^2 a_j^2]\right)} - \frac{1}{N^2} \\ &= \frac{3N\sigma^4 + 3(N^2 - N)\sigma^4}{N^2 [3N\sigma^4 + (N^2 - N)\sigma^4]} - \frac{1}{N^2} = \frac{2(N-1)}{N^2(N+2)}. \end{aligned} \quad (\text{A-2})$$

Equations (A-1) and (A-2) show that both the mathematical expectation and the standard deviation (the square root of variance) of the random noise semblance decrease at the rate of  $1/N$  with the increase in the number of traces. To derive these equations, I make an assumption that the terms in the numerator and denominator are statistically independent. Rather than proving this assumption mathematically, I test it by numerical experiments with multiple random number realizations. Figure A-1 compares the theoretical prediction with experimental measurements from 10,000 random realizations.

Applying similar analysis to the *AB* semblance (7), we deduce that

$$\begin{aligned}
E[\alpha^2(\mathbf{a})] &= \frac{E \left[ 2 \sum_{i=1}^N a_i \sum_{i=1}^N \phi_i \sum_{i=1}^N a_i \phi_i - \left( \sum_{i=1}^N a_i \right)^2 \sum_{i=1}^N \phi_i^2 - N \left( \sum_{i=1}^N a_i \phi_i \right)^2 \right]}{E \left[ \sum_{i=1}^N a_i^2 \right] \left[ \left( \sum_{i=1}^N \phi_i \right)^2 - N \sum_{i=1}^N \phi_i^2 \right]} \\
&= \frac{2 E[a_i^2] \left[ \left( \sum_{i=1}^N \phi_i \right)^2 - N \sum_{i=1}^N \phi_i^2 \right]}{N E[a_i^2] \left[ \left( \sum_{i=1}^N \phi_i \right)^2 - N \sum_{i=1}^N \phi_i^2 \right]} = \frac{2}{N}. \tag{A-3}
\end{aligned}$$

and

$$\begin{aligned}
V[\alpha^2(\mathbf{a})] &= \frac{E \left[ \left\{ 2 \sum_{i=1}^N a_i \sum_{i=1}^N \phi_i \sum_{i=1}^N a_i \phi_i - \left( \sum_{i=1}^N a_i \right)^2 \sum_{i=1}^N \phi_i^2 - N \left( \sum_{i=1}^N a_i \phi_i \right)^2 \right\}^2 \right]}{E \left[ \left( \sum_{i=1}^N a_i^2 \right)^2 \right] \left[ \left( \sum_{i=1}^N \phi_i \right)^2 - N \sum_{i=1}^N \phi_i^2 \right]^2} - \frac{4}{N^2} \\
&= \frac{2 \left[ 2 \left( \sum_{i=1}^N \phi_i \right)^2 + N \sum_{i=1}^N \phi_i^2 \right]^2 + 6 N^2 \left( \sum_{i=1}^N \phi_i^2 \right)^2 - 24 N \left( \sum_{i=1}^N \phi_i \right)^2 \sum_{i=1}^N \phi_i^2}{\left[ 3 N + (N^2 - N) \right] \left[ \left( \sum_{i=1}^N \phi_i \right)^2 - N \sum_{i=1}^N \phi_i^2 \right]^2} - \frac{4}{N^2} \\
&= \frac{4(N-2)}{N^2(N+2)}. \tag{A-4}
\end{aligned}$$

One can see that, in the case of the *AB* semblance, the mathematical expectation and the standard deviation of the random noise semblance decrease at the rate of  $2/N$ , twice higher than that for the conventional semblance. Figure A-2 compares the theoretical prediction with experimental measurements.

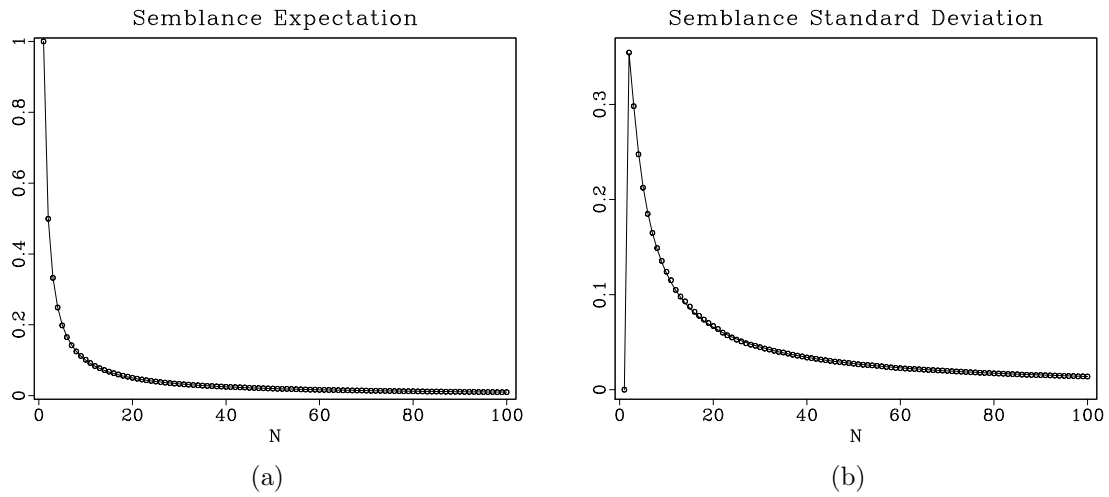


Figure A-1: Mathematical expectation (a) and standard deviation (b) of random-noise semblance as functions of the number of traces  $N$ . Solid lines are theoretical curves, circles are measurements from a numerical experiment.

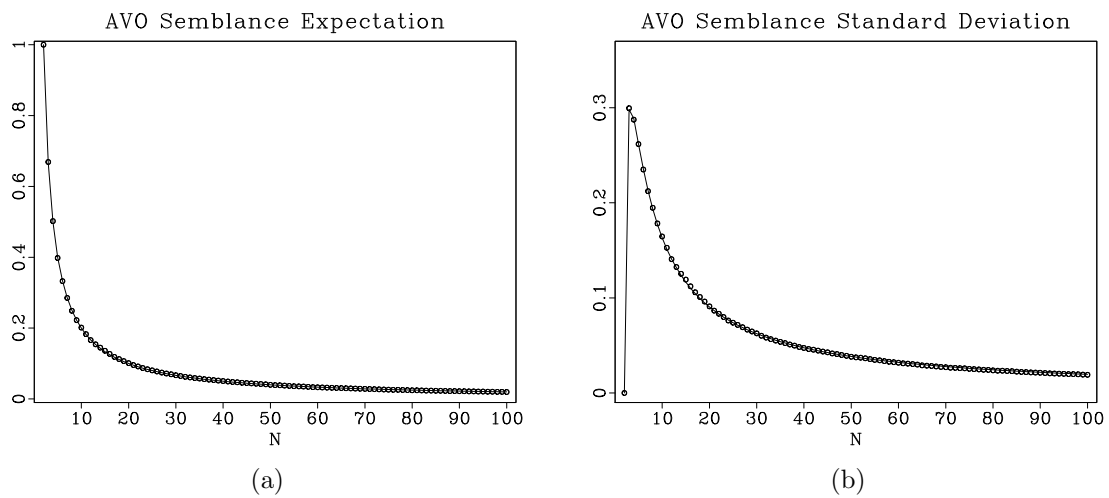


Figure A-2: Mathematical expectation (a) and standard deviation (b) of random-noise *AB* semblance as a function of the number of traces  $N$ . Solid lines are theoretical curves, circles are measurements from a numerical experiment.

## APPENDIX B

### AUTOMATIC VELOCITY PICKING FROM SEMBLANCE SCANS

The problem of automatic picking of velocities from semblance scans has been considered by many authors (Adler and Brandwood, 1999; Siliqi et al., 2003; Arnaud et al., 2004). The approach taken in this paper is inspired by the suggestion of Harlan (2001) to look at velocity picking as a variational problem. According to Harlan (2001), an optimally picked velocity trend  $v(t)$  in the semblance field  $\alpha(t, v)$  corresponds to the maximum of the variational integral

$$P_1[v(t)] = \int_{t_{min}}^{t_{max}} \alpha(t, v(t)) dt . \quad (\text{B-1})$$

I take the variational formulation further by considering its analogy to the ray tracing problem. The first-arrival seismic ray is a trajectory corresponding to the minimum traveltime. The trajectory corresponding to an optimal velocity trend should minimize an analogous measure defined in the space of the velocity scan  $\{t, v\}$ . I use the variational measure

$$P_2[v(t)] = \int_{t_{min}}^{t_{max}} \exp[-\alpha(t, v(t))] \sqrt{\lambda^2 + [v'(t)]^2} dt . \quad (\text{B-2})$$

where  $\lambda$  is a scaling parameter. According to variational theory (Lanczos, 1966), an optimal trajectory can be determined by solving the eikonal equation

$$\left(\frac{\partial T}{\partial v}\right)^2 + \frac{1}{\lambda^2} \left(\frac{\partial T}{\partial t}\right)^2 = \exp[-2\alpha(t, v)] \quad (\text{B-3})$$

with a finite-difference algorithm. The quantity in the right hand side of equation (B-3) plays the role of squared slowness. Small slowness corresponds to high semblance and attracts ray trajectories in a “wave guide”. After obtaining a finite-difference solution, the picking trajectory can be extracted by tracking backward along the traveltime gradient direction. An analogous approach has been used in medical imaging in the method of virtual endoscopy (Deschamps and Cohen, 2001). To remove random oscillations, I smooth the picked trajectory using the method of shaping regularization (Fomel, 2007).

## REFERENCES

- Adler, F., and S. Brandwood, 1999, Robust estimation of dense 3-D stacking velocities from automated picking: 69th Ann. Internat. Mtg, Soc. of Expl. Geophys., 1162–1165.

- Arnaud, J., D. Rappin, J.-P. Dunand, and V. Curinier, 2004, High density picking for accurate velocity and anisotropy determination: 74th Ann. Internat. Mtg., Soc. of Expl. Geophys., 1627–1629.
- Deschamps, T., and L. D. Cohen, 2001, Fast extraction of minimal paths in 3D images and applications to virtual endoscopy: *Medical Image Analysis*, **5**, 281–299.
- Fomel, S., 2007, Shaping regularization in geophysical-estimation problems: *Geophysics*, **72**, R29–R36.
- Harlan, W. S., 2001, Constrained automatic moveout picking from semblances: <http://billharlan.com/pub/papers/autopick.pdf>.
- Lanczos, C., 1966, *The variational principles of mechanics*: University of Toronto Press.
- Ratcliffe, A., and F. Adler, 2000, Accurate velocity analysis for Class Ii AvO events: 70th Ann. Internat. Mtg, Soc. of Expl. Geophys., 232–235.
- Rutherford, S. R., and R. H. Williams, 1989, Amplitude-versus-offset variations in gas sands: *Geophysics*, **54**, 680–688.
- Sarkar, D., R. T. Baumel, and K. L. Larner, 2002, Velocity analysis in the presence of amplitude variation: *Geophysics*, **67**, 1664–1672.
- Sarkar, D., J. P. Castagna, and W. Lamb, 2001, AVO and velocity analysis: *Geophysics*, **66**, 1284–1293.
- Shuey, R. T., 1985, A simplification of the Zoeppritz-equations: *Geophysics*, **50**, 609–614. (Errata in GEO-50-9-1522).
- Siliqi, R., D. L. Meur, F. Gamar, L. Smith, J. Toure, and P. Herrmann, 2003, High-density moveout parameter fields V and Eta, Part 1: Simultaneous automatic picking: 73rd Ann. Internat. Mtg., Soc. of Expl. Geophys., 2088–2091.
- Taner, M. T., and F. Koehler, 1969, Velocity spectra - Digital computer derivation and applications of velocity functions: *Geophysics*, **34**, 859–881. (Errata in GEO-36-4-0787).
- Yilmaz, O., 2000, *Seismic data analysis*: Soc. of Expl. Geophys.